

An upper bound on the solar radar cross section at 50 MHz

W. A. Coles,¹ J. K. Harmon,² M. P. Sulzer,² J. L. Chau,³ and R. F. Woodman³

Received 9 September 2005; revised 12 January 2006; accepted 18 January 2006; published 22 April 2006.

[1] We have made 16 unsuccessful attempts, in February and October 2003, and February 2004, to observe solar echoes using the 50 MHz radar at Jicamarca in Peru. The upper bound that we have determined on the solar cross section is significantly lower than the average of earlier reported observations. In this paper we will describe the observations, discuss the noise and interference from solar bursts, and suggest possible reasons why the echo might be weaker than expected.

Citation: Coles, W. A., J. K. Harmon, M. P. Sulzer, J. L. Chau, and R. F. Woodman (2006), An upper bound on the solar radar cross section at 50 MHz, *J. Geophys. Res.*, *111*, A04102, doi:10.1029/2005JA011416.

1. Introduction

[2] The Sun was the second target attempted in the development of radar astronomy (after the Moon). The first detailed calculations of the expected echo and the radar parameters required were done by *Kerr* [1952], and echoes were first reported at 25 MHz by a Stanford group in 1959 [*Eshleman et al.*, 1960]. A dedicated 38-MHz solar radar was built at El Campo, Texas by an MIT group and regular observations were made between 1960 and 1969 [*Abel et al.*, 1961; *Chisholm and James*, 1964; *James*, 1964, 1966, 1968, 1970]. Unfortunately these observations were not fully understood, and they have not contributed much to our present understanding of the corona. Attempts were also made to observe the Sun at 50 MHz at Jicamarca in 1964 (K. Bowles, B. Balsley, and D. Farley, private communication, 2002) and at 40 MHz at Arecibo in 1968 (A. Parrish and D. Campbell, private communication, 2001). No detection was made at Jicamarca. Echoes were apparently observed at Arecibo but the detection was marginal and the data were never published. More recent reviews are given by *Rodriguez* [2000] and *Coles* [2004].

[3] In retrospect, the early observers faced several insurmountable difficulties in understanding their observations. First, the large scale structure of the corona is often dominated by features, such as coronal holes and coronal mass ejections (CMEs), which were unknown at the time. Second, the microstructure which governs the angular spread of the backscattered radiation was unknown. Third, the radar reflection point is at the base of the solar wind, which had just been discovered and was largely unknown. Finally, they did not have simultaneous optical observations to help constrain the coronal geometry. Eventually interest

in the solar observations waned, the El Campo radar was scrapped, and radar astronomy evolved towards the use of higher frequencies. Higher frequencies penetrate through the transition region into the cool dense plasma of the chromosphere where they are heavily attenuated, so it became impossible to repeat the observations and solar radar has been almost forgotten.

[4] Solar physicists have realized for some time that new solar radar observations with modern signal processing, dual polarization, and multiple frequencies, combined with modern optical, UV, and X-ray observations, could make a significant contribution to the fundamental questions of coronal heating and solar wind acceleration. Such observations were also expected to provide an early warning of Earth-directed CMEs which are otherwise difficult to detect. However, the cost of building a radar like El Campo would be too high to justify without a demonstration of feasibility. We realized recently that the planned ionospheric heater for Arecibo could be used as a solar radar with minor modifications. The observations to be discussed here were an attempt to revive the technique before the Arecibo heater became available. Solar radar observations at frequencies above 25 MHz are possible at present only at Jicamarca. Lower frequency observations may be possible at various installations, but they will suffer strong ionospheric scintillations.

[5] The radar cross section measured at El Campo was roughly the cross sectional area of the Sun (at the reflection height), as expected, but it was much more variable than expected. Furthermore there was no sign of a specular reflection. The doppler width was about 30 KHz and there was a positive doppler shift of the order of 20 KHz. The delay depth of the Sun is about 10 s, so they used a delay resolution of 0.5 s and decoded 20 delay samples around the expected mean delay. They used a code period of 127 samples. Echoes were found throughout the entire range, but were concentrated at a height of about 1.5 solar radii as expected. *James* [1964] and colleagues were unable to find any strong and consistent correlation with solar observations, although correlations were reported by other workers [*Gerasimova*, 1974]. Subsequent analyses were unable to

¹Electrical and Computer Engineering, University of California at San Diego, La Jolla, California, USA.

²National Astronomy and Ionosphere Center, Arecibo, Puerto Rico, USA.

³Radio Observatorio de Jicamarca, Instituto Geofísico del Perú Lima, Peru.

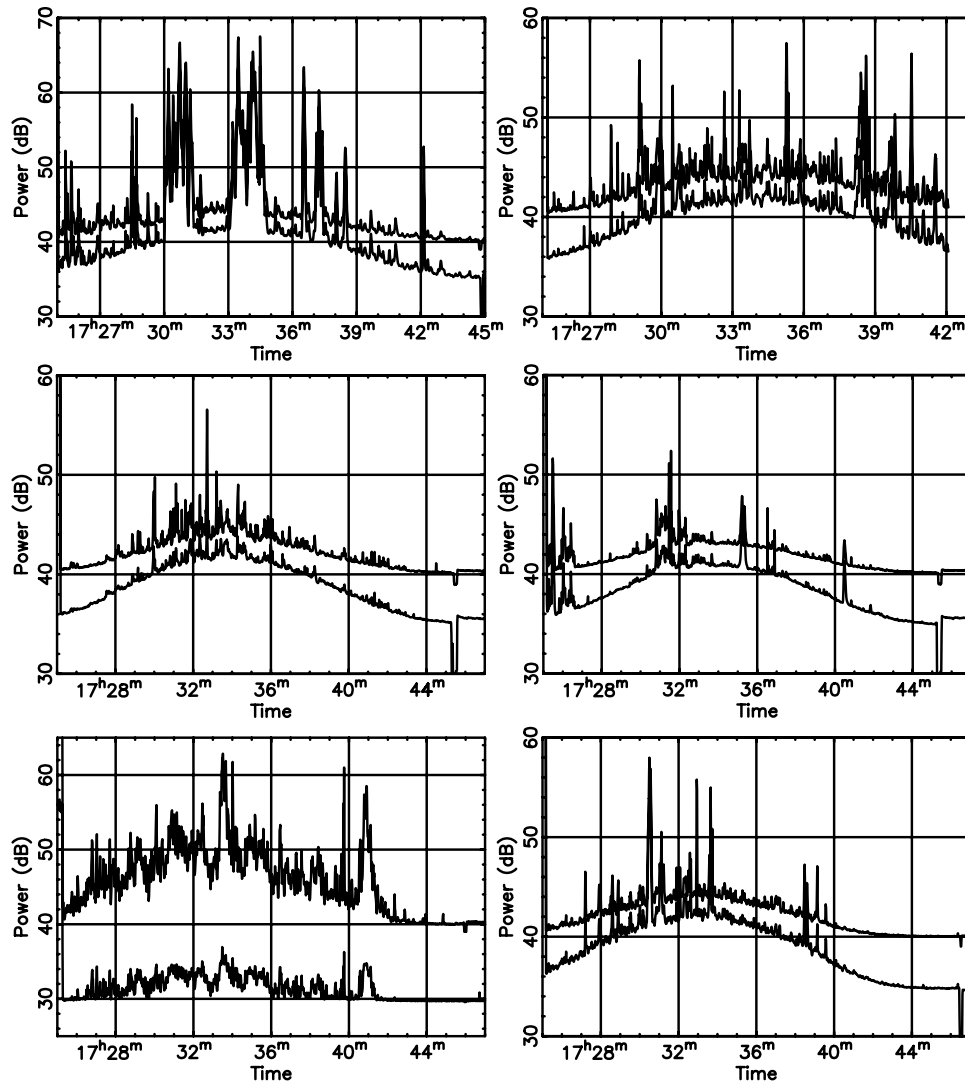


Figure 1. Total power in two polarizations 10–15 February 2004. The upper trace is RHC, and the lower is LHC on each day. The date runs left to right, then top to bottom. The bandwidth $B = 1$ MHz and integration time $T = 1$ s. On this plot the theoretical thermal radiometer noise would be 0.013 dB rms or roughly 0.1 dB peak to peak.

find a correlation between changes in the El Campo data and coronal observations [Owocik *et al.*, 1982]. Most troublesome is the lack of any sign of the 27 day solar rotation period in the radar observations because this period is visible in most coronal observations. Several unpublished attempts have been made to correlate the high amplitude echos with signs of coronal mass ejections such as sudden ionospheric commencements (P. Rodriguez, private communication, 2003; T. van Eyken, private communication, 2003), but no such correlation was found.

[6] The dominant feature of solar observations at meter wavelengths is strong and highly variable solar nonthermal noise. The brightness temperature of the quiet Sun at 50 MHz is of the order of 10^6 K, and bursts of nonthermal noise can exceed the total flux of the quiet Sun by a factor of 100. This noise is shown very clearly in Figure 1, which displays the total power records from our February 2004 observations. During this period the solar activity was categorized as “low” to “very low” by the Space Environment Center. Even during this quiet period the noise is

dominated by bursts. This was, of course, recognized by early radar observers [James, 1964, 1970]. Solar bursts are the dominant consideration in design of the data analysis algorithms, not only because they greatly increase the noise level, but because they can cause a spurious echo.

[7] The following sections cover: (2) the observing configuration; (3) the data analysis; and (4) the results. These sections are more detailed than normal because our results are negative; we did not detect any echoes even though the sensitivity of our experiment was comparable with that of James [1970]. It is, of course, possible that we made a blunder in the experiment, so we have described it in more detail than usual. The final section (5) provides a discussion of the implications of our negative results.

2. Jicamarca System Configuration

[8] The solar echo, as observed by James [1970], is highly overspread in the sense that its bandwidth is 30 KHz, so its coherence time is 30 μ s, whereas the

delay resolution is hundreds of ms. The echo is incoherent between delay bins. This means that phase coding is not possible and one must use a code which does not require phase coherence, such as pulse amplitude modulation (PAM) or frequency shift keying (FSK). The received signal must first be spectrum analyzed, conceptually it is as if one were using a filterbank receiver where each channel has a square law detector on its output. The decoding is done by correlating the detected power in each channel with the transmitter modulation code. In a coherent system the same virtual filterbank would be used but without a square law detector, and the correlation would be with the transmitted voltage not the power. Incoherent decoding does not provide the linear “code gain” that one can obtain with coherent decoding, the signal-to-noise ratio increases only as the square root of the code length. Incoherent decoding is also more sensitive to noise, particularly impulsive positive-definite noise. If the transmitter bandwidth is sufficient, FSK provides 41% better signal to noise ratio than PAM because the transmitter is on all the time.

[9] The signal-to-noise ratio (SNR) of a solar radar is determined by the flux that the radar can deliver to the Sun, and the noise of the Sun itself. The received signal flux S_r is determined by the transmitter power P_t ; the transmitting antenna area A_t and gain $G_t = 4\pi A_t/\lambda^2$; and the solar radar cross section σ_r . The solar noise flux S_s in each polarization is determined by the solar temperature T_s ; the solar cross section σ_s ; the solid angle subtended by the Sun at the Earth $\Omega_s = \sigma_s/R^2$; the bandwidth B , and the wavelength. The signal undergoes some loss L_p in the lower corona, which is estimated to be about 3 dB at 50 MHz [James, 1970]. Recent work suggests that this loss might be somewhat underestimated (G. Price, private communication, 2002) because the collision frequency is not accurately calculated. If the transmitter and receiver beams are broader than the Sun (as is true for Jicamarca and El Campo), then we can estimate the signal-to-noise ratio as follows.

$$\begin{aligned} S_r &= P_t G_t L_p \sigma_r / (4\pi R^2)^2 \\ S_s &= k T_s \Omega_s B / \lambda^2 \\ \text{SNR} &= P_t A_t L_p \sigma_r / (4\pi R^2 k T_s B \sigma_s) \end{aligned} \quad (1)$$

The area of the receiving antenna and the noise temperature of the receiver are irrelevant, provided only that the solar noise exceeds the galactic background. From this expression one can see that the appropriate figure of merit to compare different radars is the power-area product.

[10] The whole Jicamarca array could not be used for both transmitting and receiving in this experiment because the beam width is too narrow to use the same beam for transmitting and receiving and there was not sufficient time to change the pointing direction between transmitting and receiving. However, the quadrants can be configured independently. In February 2003 we used two quadrants to transmit and two to receive because this did not require a change in the transmitter manifold. However, in October 2003 and February 2004 we used three quadrants for transmitting and one for receiving. This allowed us to use the three available power amplifiers,

one for each of the transmitting quadrants. The physical area of each quadrant is 20,000 m² and the aperture efficiency is 66%. The total average (CW) power is 80 KW. So the power aperture product is 3.17×10^9 w m² as configured for this experiment. The El Campo system had an effective area of 20,000 m² and CW power of 500 KW. However, it was not normally pointing directly overhead so the average efficiency was about 75%. The power aperture product was 7.5×10^9 w m². Jicamarca has two polarizations, which increases the sensitivity by 41% if the echo is unpolarized (as we expect). El Campo also had two polarizations. The transmitter was connected to one linear polarization and the other, which had only half the area, was used only for receiving.

[11] The longest transmitter pulse possible at Jicamarca is 2 ms. We used this pulse length in February 2003, with the hope of discovering fine structure if it existed. We did not see any echo, so in subsequent observations we switched to synthesizing a CW signal using a train of 0.5-ms pulses with a 10-ms interpulse period (IPP). We then FSK modulated this pseudo-CW signal at a baud of 400 ms. Using shorter pulses in the “CW” signal gave less power supply droop, so the transmitter was more stable and the mean power was higher. We used the maximum FSK shift that was compatible with the transmitter tuning. We started with 250 KHz and reduced it to 200 KHz obtaining a small increase in transmitted power and better power balance between the two FSK frequencies.

[12] The transmitting quadrants were configured to transmit left-hand circular polarization (LCP) so that we could determine the cross polarization if we detected an echo. The receiving quadrant could have been sampled as orthogonal linear polarizations, but we chose to insert a quadrature hybrid and sample the two circular polarizations. This eliminated the need to calibrate the preamplifier gain and phase in both channels.

[13] The February 2003 observations were done with analog receivers, the October 2003 observations with digital and analog receivers in parallel, and the February 2004 observations with only digital receivers. The digital receivers had better dynamic range and a broader and much more uniform IF passband than the analog receivers. However, neither of the receivers were designed for continuous sampling because this is not necessary for an incoherent scatter radar. A 3 μ s data gap was inserted every IPP to allow transfer from the digital receiver to the pc memory. A 30 ms gap was inserted every 8 s to allow transfer from pc memory to disc. These gaps are a very small fraction of the total time and individually small compared with the code baud (400 ms), so we filled them with random data to provide a continuous time series.

[14] The digital receiver was controlled by a pc running MS Windows, and the operating system sometimes extended the 30-ms data gaps to 40 ms in a quasi-random way. This jitter was small compared with the code baud, but the resulting uncertainty led us to design a synchronization mechanism for the February 2004 observations. The transmitter controller continued to run during the receive period and the IPP is controlled by the station master clock, so we inserted a 10- μ s burst of transmitter signal in every IPP at the sampler. This was switched in exactly the same phase of every IPP cycle, so it was easy to check and easy to gate out

of the data series. Since it was coded we could reconstruct the time modulo the 25.2-s code period.

3. Observations and Data Analysis

[15] Observations were made during five days in February 2003, five days in October 2003, and six days in February 2004. In February 2003 the system was optimized for delay resolution between 2 and 40 ms. No echoes were detected, which we assume is because the echo has very little power at this scale. In October 2003 the Sun was unusually active, so our upper bounds are not as tight as those obtained on 10–15 February 2004. We will discuss only the February 2004 data here because the system worked well throughout and the Sun was relatively quiet. However, it is interesting and unfortunate that we were unable to observe the largest coronal mass ejection in the last 30 years (the famous “Halloween storm” of 28 October), which was traveling towards the Earth, because the associated flares increased the system noise enormously. This suggests that the solar radar technique will always have difficulty observing such transients, which compromises the value of the technique for “space weather” forecasting.

[16] The radio source Hydra was observed on 5 February with both linear polarizations of each quadrant. Before and after the observation each antenna input was replaced with a noise generator. In this way we estimated the effective area of each of the eight subarrays. The Sun was observed on 9 February with all quadrants phased for the radar observations. This confirmed that the subarrays had been phased correctly. The power in the transmitting quadrants peaked about 1000 s before the power in the receiving quadrants, as planned.

[17] The antenna pointing was adjusted twice during the 6 days of observation, so we first computed the total power integrating over the whole system bandwidth and fit that data to estimate the beam center and beamwidth for the receiving quadrant. We could not fit the transmitting beam shape directly because we had to remove the TR switches to reconfigure the transmitting manifold. Thus we used the computed shape for the transmitting beam.

[18] The delay-doppler analysis was done in a simple and straightforward way. The data were broken into 2048 sample blocks and Fourier transformed. These blocks are 2-ms long, and the transform has 500-Hz resolution. The squared magnitudes of the Fourier transforms were computed and adjacent frequencies were summed to reduce the spectral resolution to 1 KHz. The spectra were then averaged into 400-ms bins. This is equivalent to passing the receiver signal through a 1024 channel filter bank with total width 1 MHz, where each channel is followed by a square law detector and a 400 ms integrator. These bins were then correlated with the 63-length pseudo-random transmitter code. The bins were also summed to provide a measure of the mean noise spectrum, which was then used to normalize the delay-doppler distribution. Each frequency channel was decoded individually, as if the modulation had been amplitude modulated (on or off) according to the transmitter code, and normalized by the mean noise power in that channel. Since the transmitter was actually FSK modulated, an echo would appear as a positive bump at one frequency and a negative bump at a frequency separated by exactly the FSK

shift. The final FSK delay-doppler distribution was obtained by shifting the PAM distribution by the FSK shift (250 or 200 KHz) and subtracting the shifted distribution from the original.

[19] The process of averaging into 400-ms bins, i.e., post detection smoothing, was done with optimal noise weighting. The optimal weight, assuming the signal is constant and the noise varies, is the inverse of the noise variance. Since the signal is much weaker than the noise, we use the observed power as an estimate of the rms noise. We first divided by the transmit and receive beam gains to make the signal constant, then we divided by the square of the mean observed power. The mean power was determined by integrating over the receiver bandwidth, since the noise was broadband.

[20] To synchronize the code, we first computed a delay-doppler distribution from a single code period at the start and another at the end of the transmitting interval. This confirmed the phase of the transmitter code and the effective IPP. We then computed another delay-doppler plot from a code period at the end of the receive interval. The calibration signal confirmed that the synchronization persisted through the receive interval. Once the code was synchronized and the effective IPP known, we analyzed the receive interval, with the calibration signal gated out, using optimal noise weighting.

[21] The pseudo-random codes are designed to have an autocorrelation function which is close to ideal. The sidelobes are all $-1/N$, where N is the code length. When the signal is modulated with the optimal noise weighting function the code no longer has such nice sidelobes. We have measured the autocorrelation of the weighted code with the ideal code using the calibration signal. An example is shown in Figure 2 below. It appears that the sidelobes become a random process with a standard deviation of $1/N$. This would be a problem if the signal-to-noise ratio were high, but that is not the case with our observations.

4. Results

[22] A typical delay-doppler plot of the signal-to-noise ratio with optimal weighting is shown in Figure 3 below. This is the RCP from 10 February 2004. We have outlined the limits of the El Campo delay-doppler window. The doppler resolution has been smoothed to 11 KHz but the delay resolution remains 400 ms. The rms noise (σ) in this plot is about 50% higher than that expected from solar thermal noise, and a 4σ peak can be seen precisely where an echo might be expected. However, this peak can be shown to be a result of leakage of the calibration signal through the electronic switch (at a level of -55 dB). The 4σ peak has only about 10% of the energy expected in the echo. The matching LCP, shown in Figure 4 below, is similar but there is no calibration leakage.

[23] The noise statistics in the delay-doppler plot are different in delay and doppler. The delay samples are independent but the doppler samples are not. The delay decoding consists of cross correlating the received signal with the pseudo-random delay code. The noise spectrum has thus been whitened on the delay axis by the multiplication with the white delay code. However, the spectrum of the noise on the doppler axis is not modified by the decoding. We

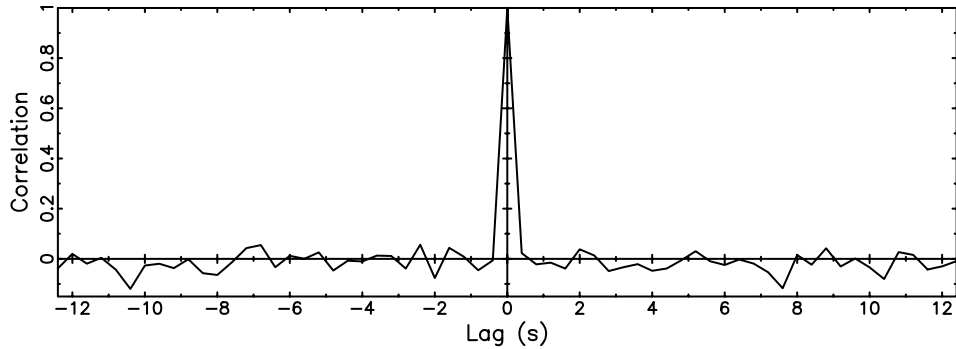


Figure 2. Cross correlation of the weighted calibration signal with the transmitted code using the weights for 11 February 2004.

confirmed this by computing the autocorrelation of the delay-doppler distribution shown in Figure 4. Cuts through the two-dimensional autocorrelation are shown in Figure 5. The cut along the delay axis shows only a delta function at the origin, as expected. The cut along the doppler axis of the autocorrelation shows two roughly equal components. One, the spike at the origin, is the thermal noise. The other is evidently leakage from the non-stationary nonthermal noise.

[24] At the basic doppler resolution of 1 KHz the noise is dominated by thermal noise. When the doppler resolution is broadened to 11 KHz by smoothing, the thermal and nonthermal components are roughly equal. When the doppler resolution is further broadened the nonthermal component dominates the noise. Thus further smoothing degrades the sensitivity to echoes which have width less than 11 KHz, and does not reduce the total noise much.

[25] The effect of optimal noise weighting can be calculated because the nonthermal noise can be so impulsive that

there are some times when it is negligible. From these we can estimate the underlying thermal noise and thus the “ideal” signal to thermal noise ratio. We can then compare this with the signal-to-noise ratio that one would obtain using different weighting schemes. Using the actual data displayed in Figure 3, we find that the optimal weighting gives an SNR (rms) which is 60% of the ideal thermal SNR. If we had simply weighted the same data uniformly, the SNR would have been only 1% of the ideal SNR. Thus the nonthermal noise is not as prohibitive as one might expect on viewing Figure 1; it does not even halve the SNR when optimally processed. However, it tends to mimic the expected echo because of its spectral coherence.

[26] All of our observations show features which could be interpreted as echoes, i.e., they are narrow in delay and have a width of 30 to 50 KHz in doppler as do those reported by the El Campo group. An example is shown in Figure 6. Here there is a feature in the box representing the El Campo

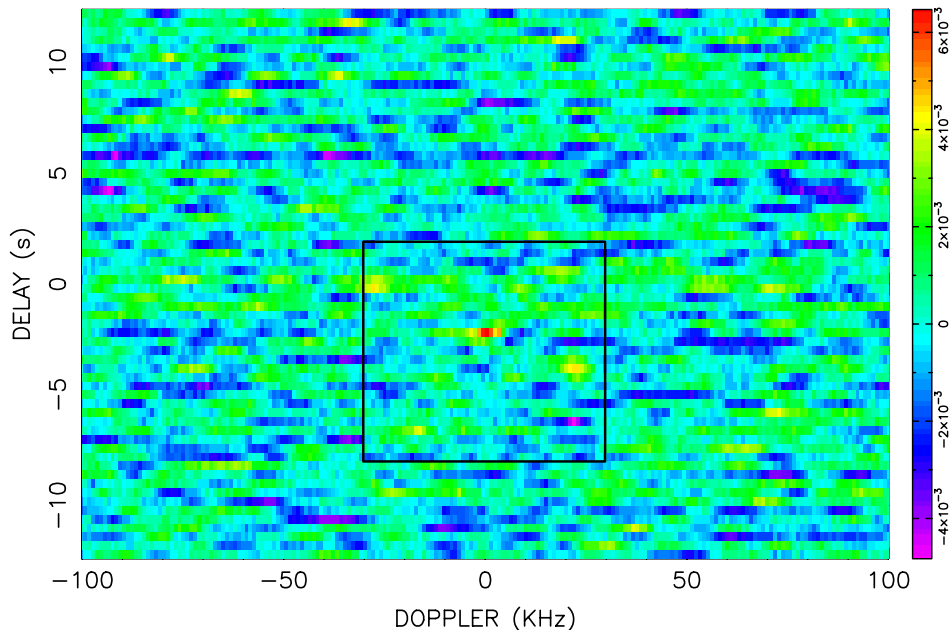


Figure 3. Delay-doppler distribution of the signal-to-noise ratio with optimal weighting for RCP on 10 February 2004. The apparent signal at zero doppler and 2 s before the Sun is leakage from the calibration signal. The expected echo has about 10 times the area of this leakage. The box represents the El Campo limits.

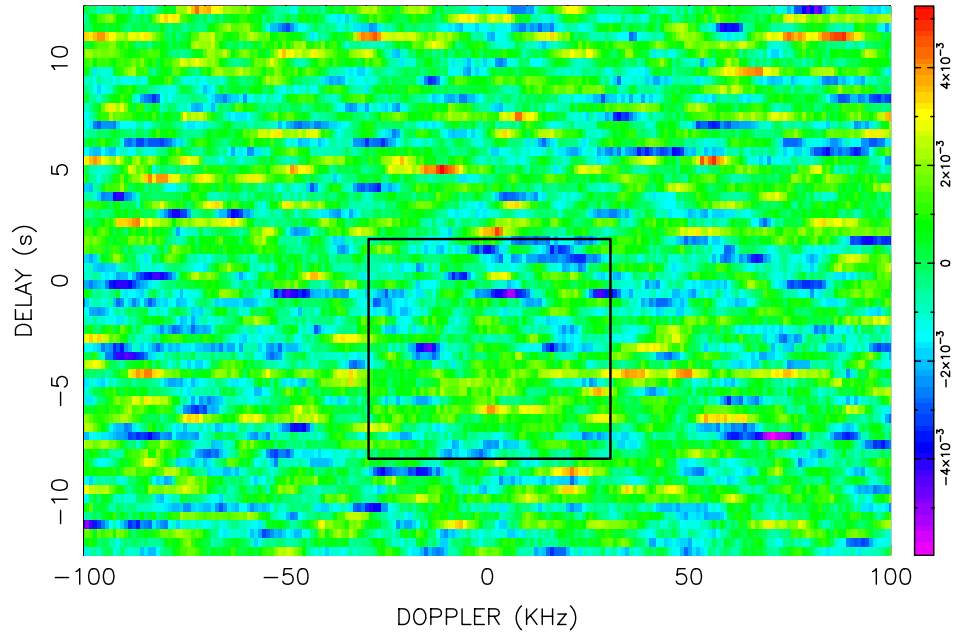


Figure 4. Delay-doppler distribution for LCP on 10 February 2004. There is no calibration signal in this polarization.

window, but there are more features of the same amplitude and shape above the box, i.e., behind the Sun.

[27] Another example is shown in Figure 7. Here there is a large feature to the right above the box. Although we did not expect an echo from behind the Sun, and none were reported at El Campo, we considered the possibility. We analyzed this observation by successive bisection of the data, and eventually discovered that the echo was confined to a 30 s interval. There was no burst or peculiarity in the total power during that interval, but the feature could not be a true echo because its cross section would have to be enormous to be so visible in 30 s.

[28] Unfortunately all our “candidate” echoes can be discarded for various reasons. The delay-doppler distributions are very homogeneous, it is impossible to tell from the data where the Sun is located. There is no evidence for any real echo at the 4σ level. If, during the 6 days observed in February 2004, the radar cross section of the Sun had been 10% of the physical cross section then we would have observed it. Thus there appear to be extended periods when the solar cross section is less than 10% of the average of the El Campo observations. The cross section measurements at El Campo did occasionally drop to 10% of the average, but the cross section appeared to be independent from day to day and there are no reported periods of prolonged low cross section.

[29] We cannot analyze our data exactly as James and colleagues were forced to do because we cannot duplicate their analog signal processing, particularly the nonlinear gain control described by James [1968]. However, if we removed our optimal weighting, we would find apparent echoes very similar to those they have reported. Even with optimal weighting we find apparent echoes, but they are distributed uniformly in our much larger delay-doppler window. We know these apparent echoes are spurious and we have traced their origin to impulsive solar noise “leak-

ing” through our radar decoder. Thus we are confident that some of the reported measurements at El Campo were spurious, but we cannot say that all the El Campo measurements were spurious.

5. Discussion

[30] Some discussions of possible radar reflection mechanisms have appeared in the literature since the El Campo observations were terminated [Mel’Nik, 1999; Chashei and Shishov, 1994; Wentzel, 1981; Gordon et al., 1971; Gordon, 1971], but since there have been no new observations the theoretical suggestions cannot be verified. These mechanisms all predicted the signal that was apparently observed, so they are not particularly helpful in understanding our

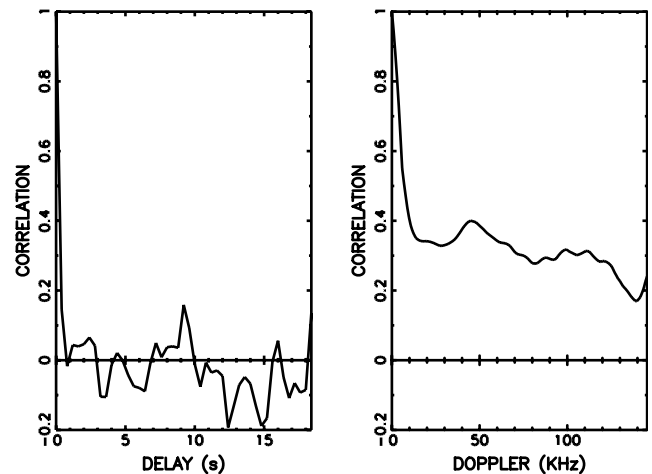


Figure 5. Cuts through the autocorrelation of the delay doppler distribution shown in Figure 4. Here the doppler resolution is 11 KHz.

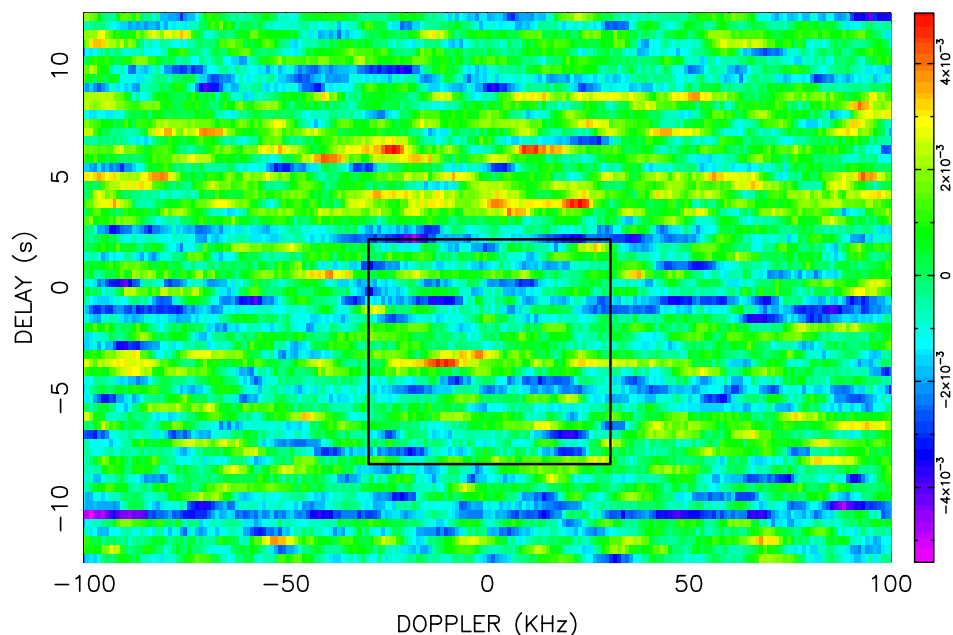


Figure 6. Delay-doppler distribution for LCP on 11 February 2004.

results which indicate that it is often much weaker. There are at least three mechanisms which would reduce the radar cross section significantly below the solar cross section. One is simply the coronal geometry at the minimum of solar activity. This is dominated by a closed field arcade around the equator and polar coronal holes covering most of the disc. The incident radar wave would be reflected by the center of the arcade, but where the wave hits the side of the arcade it would be reflected down into the polar hole, which would have much higher attenuation because the reflection height is much lower. Two other plausible mechanisms for reducing the echo power were proposed by *Coles*

[2004], and both could operate. First, the attenuation in the corona could be much higher than calculated because the incident radar wave will not encounter a smooth reflecting surface, rather a deeply modulated one. Thus it will spend a much longer time close to the critical surface than otherwise. This can substantially increase the loss. Second, the incident wave will be reflected from outwards traveling density irregularities. If these are moving with the solar wind flow velocity, then the echo will not be strongly doppler shifted or broadened. However, if the density irregularities are caused by outwards propagating compressive MHD waves, as has been proposed [*Harmon and*

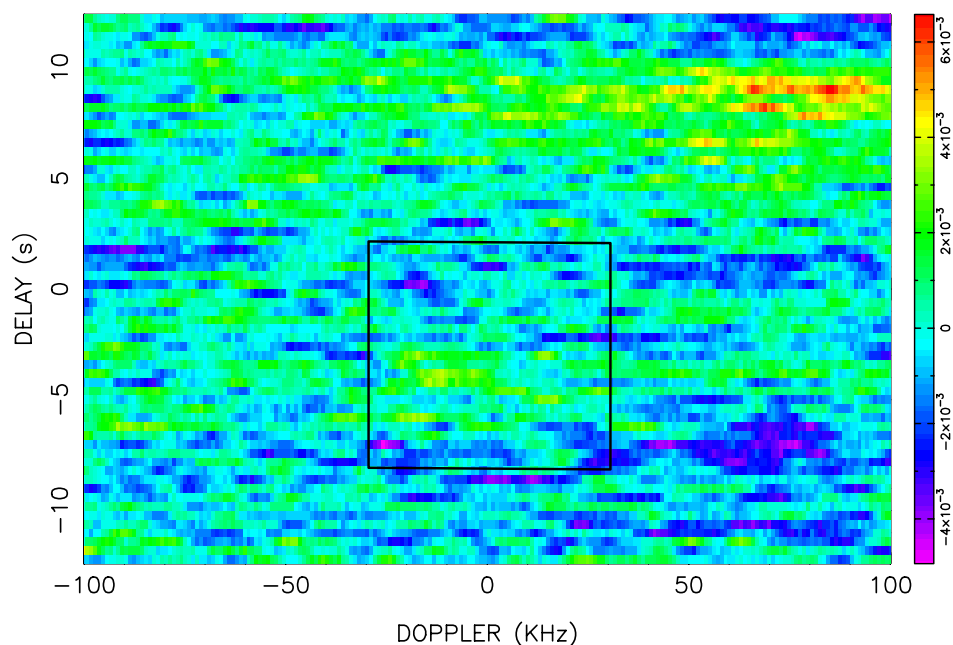


Figure 7. Delay-doppler distribution for LCP on 12 February 2004.

Coles, 2005], then the doppler shift and broadening will be a factor of 10 larger. In that case the echo amplitude would be reduced by a factor of 10 and we would not be able to detect it. Both of these mechanisms would also affect the El Campo data, so they explain why our upper bound is lower than expected, but they do not explain why the El Campo observations are roughly as expected. It is also possible that the solar radar cross section has a strong frequency dependence, because the 26.5-MHz observations at Stanford were more than a factor of 10 stronger than the average echoes at El Campo. This could happen if the coronal electron density and temperature were lower than expected so the reflection point was closer to the transition region (G. Price, private communication, 2002). Then our 50-MHz observations might be expected to be a factor of 10 weaker than those at El Campo. The electron temperature is not easy to measure, but the required densities and temperatures are at the bounds of the plausible range.

[31] We must also consider the possibility that many of the reported observations at El Campo were spurious. Evidence for this is clear in our data. This consideration is strengthened by the work of *Gerasimova* [1974], who reports that the strongest correlation with enhanced echo cross section was with Type III storms. There is little correlation between Type III storms and large scale coronal structure, but it was Type III storms that leaked into our delay-doppler spectra and caused pseudo-echoes. This possibility is further strengthened by the absence of significant autocorrelation at the solar rotation period of 27 days.

[32] It would be very interesting to repeat the experiment with a more powerful transmitter. For example, the proposed Arecibo heater with a 1-MW transmitter operating at 25 MHz, would increase the power-aperture product by a factor of 5. A multi-beam receiving array such as LOFAR (<http://www.lofar.org>), which is now under construction in the Netherlands, would provide spatial resolution of the echo. This would be extremely valuable scientifically, but the signal to noise ratio in each beam would not be much higher than that of a smaller antenna unless the echo power were concentrated in a few beams. The transmitter flux delivered to the Sun remains the limiting factor.

[33] In summary, our observations suggest that solar radar echoes at 50 MHz are often at least a factor of ten weaker than had been theoretically expected and apparently confirmed with the El Campo radar. It seems likely that many of the echoes apparently observed with the El Campo radar were spurious. There are several plausible theoretical mechanisms that would reduce the echo strength by at least this factor, so we must take the suggestion seriously. It will not be possible to distinguish between the various mechanisms until echoes are reliably measured with a radar system significantly more sensitive than El Campo or Jicamarca.

[34] **Acknowledgments.** We wish to thank Sixto Gonzales of NAIC for helping to facilitate the observations, and the staff of JRO for their outstanding efforts. In particular the help of Otto Castillo, Darwin Cordova, Gabriel Michhue, Marco Milla, Pablo Reyes, and Danny Scipión was essential. The Jicamarca Radio Observatory is a facility of the Instituto Geofísico del Perú and is operated with support from the NSF cooperative agreement ATM-0432565 through Cornell University.

[35] Shadia Rifai Habbal thanks V. Melnik and T. van Eyken for their assistance in evaluating this paper.

References

- Abel, W. G., J. H. Chisholm, P. L. Fleck, and J. C. James (1961), Radar reflections from the Sun at very high frequencies, *J. Geophys. Res.*, *66*, 4303.
- Chashei, I. V., and V. I. Shishov (1994), Volume scattering model of interpretation of solar radar experiments, *Sol. Phys.*, *149*, 413–416.
- Chisholm, J. H., and J. C. James (1964), Radar evidence of solar wind and coronal mass motions, *Astrophys. J.*, *140*, 377.
- Coles, W. A. (2004), Solar radar, in *Solar and Space Weather Radiophysics*, chap. 16, edited by D. E. Gary and C. Keller, Springer, New York.
- Eshleman, V. R., R. C. Barthle, and P. B. Gallagher (1960), Radar echoes from the Sun, *Science*, *131*, 329–332.
- Gerasimova, N. N. (1974), Comparison of results of radar studies of the corona with solar activity, *Sov. Astron.*, *18*, 482–485.
- Gordon, I. M. (1971), Radar observations of the Sun and a mechanism for producing the reflected signal in the corona, *Sov. Astron.*, *12*, 796–805.
- Gordon, I. M., V. A. Liperovskii, and V. N. Tsytovisk (1971), Turbulence spectra of the solar coronal plasma and the structure of a radar signal, *Sov. Astron.*, *15*, 54–63.
- Harmon, J. K., and W. A. Coles (2005), Modeling radio scattering and scintillation observations of the inner solar wind using oblique Alfvén/ion cyclotron waves, *J. Geophys. Res.*, *110*, A03101, doi:10.1029/2004JA010834.
- James, J. C. (1964), Radar echoes from the Sun, *IEEE Trans. Antennas Propag.*, *AP-12*, 876–891.
- James, J. C. (1966), Radar studies of the Sun at 38 MHz, *Astrophys. J.*, *146*, 356.
- James, J. C. (1968), Radar studies of the Sun, in *Radar Astronomy*, chap. 7, edited by J. V. Evans and T. Hagfors, McGraw-Hill, New York.
- James, J. C. (1970), Some observed characteristics of solar radar echoes and their implications, *Sol. Phys.*, *12*, 143–162.
- Kerr, F. J. (1952), On the possibility of obtaining radar echoes from the Sun and planets, *Proc. IRE*, *40*, 660–666.
- Mel’Nik, V. N. (1999), On the plasma theory of reflection of a radar signal from the Sun, *Astron. Lett.*, *25*, 336–340.
- Owocki, S. P., G. A. Newkirk, and D. G. Sime (1982), Radar studies of the non-spherically symmetric solar corona, *Sol. Phys.*, *78*, 317–331.
- Rodriguez, P. (2000), Radar studies of the solar corona: A review of experiments using HF wavelengths, in *Radio Astronomy at Long Wavelengths*, *Geophys. Monogr. Ser.*, vol. 119, pp. 155–165, AGU, Washington, D. C.
- Wentzel, D. G. (1981), A new interpretation of James’ solar radar echoes involving lower-hybrid waves, *Astrophys. J.*, *248*, 1132–1145.

J. L. Chau and R. F. Woodman, Radio Observatorio de Jicamarca, Instituto Geofísico del Perú, Lima 13, Perú. (jchau@jro.igp.gob.pe; ronw@geo.igp.gob.pe)

W. A. Coles, Electrical and Computer Engineering, University of California at San Diego, 9500 Gilman Drive, La Jolla, CA 92093-0407, USA. (bcoles@ucsd.edu)

J. K. Harmon and M. P. Sulzer, National Astronomy and Ionosphere Center, Arecibo 00612, Puerto Rico, USA. (harmon@naic.edu; msulzer@naic.edu)